Chemosphere 199 (2018) 122–129

Contents lists available at ScienceDirect

Chemosphere

journal homepage: www.elsevier.com/locate/chemosphere

Time-dependent disturbances of chloride salts on overall redox reaction and luminescence in *Vibrio fischeri*

Zhenyang Yu [c, d], Jing Zhang [a, b, *], Meifang Hou [a]

[a] College of Ecological Technology and Engineering, Shanghai Institute of Technology, Shanghai, 201418, PR China
[b] Guangxi Key Laboratory of Electrochemical and Magnetochemical Functional Materials, Guilin, 541004, PR China
[c] College of Environmental Science and Engineering, Tongji University, Shanghai 200092, PR China
[d] Jiaxing Tongji Institute for Environment, Jiaxing, Zhejiang Province, 3014051 PR China

HIGHLIGHTS

- KCl, $MgCl_2$ and $CaCl_2$ stimulated NADH and NADPH in *Vibrio fischeri*.
- Stimulations by salts increased in a time-dependent fashion.
- FMN, ATP and their genes showed time-dependent stimulation or upregulation.
- The greatest maximum biochemical stimulation is $CaCl_2 > MgCl_2 > KCl$.
- The NADH:NADPH ratios in $CaCl_2$ decreased over time.

ARTICLE INFO

Article history:
Received 14 July 2017
Received in revised form
1 February 2018
Accepted 5 February 2018
Available online 7 February 2018

Handling Editor: Jian-Ying Hu

Keywords:
Chloride salts
Redox reaction
Stimulation
Vibrio fischeri

ABSTRACT

The redox state of NADH/NADPH balance (nicotinamide adenine dinucleotide/nicotinamide adenine dinucleotide phosphate) is crucial in cellular homeostasis. Recent studies reported that sodium halide ions (NaX, X = F^-, Cl^-, Br^- and I^-) stimulated NAD(P)H in *Vibrio fischeri* (VF). However, it remained unanswered whether this pattern applied in salts with other cations, *e.g.*, K^+, Mg^{2+} and Ca^{2+}, whose aquatic concentrations were increased by anthropogenic activities and climate change. Currently, VF were incubated with chloride salts, including KCl, $MgCl_2$ and $CaCl_2$, and effects were measured in a time-dependent fashion. Both NADH and NADPH showed stimulation that increased over time, and the greatest maximum stimulation at 24 h was $CaCl_2 > MgCl_2 > KCl$. The changes of NADH/NADPH ratios over time in $CaCl_2$, $MgCl_2$ and KCl were descendent, ascendant and stable, respectively. Simultaneously, FMN:NAD(P)H reaction catalyst (luciferase, in the form of expression levels of *lux* A and *lux* B), adenosine triphosphate and the expression levels of its regulating gene *adk* were also stimulated. The luminescence showed even more significant stimulations than the overall redox reaction. Together with earlier reported effects of NaCl, the chloride salts commonly disturbed the redox state and influenced the adaption of organisms to challenging environments.

1. Introduction

Inorganic salts widely exist in environmental matrices (NRC, 2006; Dugo et al., 2007), and they are essential in osmotic pressure maintenance (Luo and Roux, 2010) and molecular interaction (Gonçalves-de-Albuquerque et al., 2017). Yet, the inorganic salts can cause hazards at excessive concentrations, provoking salt stress on both terrestrial and aquatic organisms and human beings (Fahmi et al., 2011; Bloetscher et al., 2016). In recent decades, the concentrations of inorganic salts in aquatic systems increased due to anthropogenic activities (*e.g.*, mineral mining, wastewater irrigation and effluent discharge from seawater usage for drinking water treatment) and climate change (snow melting and seawater intrusion) (Singh, 2015; Bloetscher et al., 2016; Stancanelli et al., 2017). Accordingly, the adverse effects and underlying mechanisms of inorganic salts need comprehensive investigations.

The redox state is essential in energy production and intermediary metabolism that is crucial in cellular health. The nicotinamide

* Corresponding author. College of Ecological Technology and Engineering, Shanghai Institute of Technology, Shanghai, 201418, PR China.
E-mail address: zhjshy@163.com (J. Zhang).

https://doi.org/10.1016/j.chemosphere.2018.02.029
0045-6535/

adenine dinucleotide (NAD^+/NADH) and nicotinamide adenine dinucleotide phosphate ($NADP^+$/NADPH) redox couples commonly exist in organisms from photobacteria (Jablonski and Deluca, 1978) to mammals (Blacker et al., 2014). The NADH couple drives ATP production by glycolysis and oxidative phosphorylation, and the NADPH one governs biosynthetic pathways, free radical generation and antioxidant defense (Ying, 2008; Collins et al., 2012). The NADH/NADPH were also involved in the adaptive responses of organisms to challenging environments including salinity changes (Srivastava et al., 2008; Camejo et al., 2013). Yet, the responses of NAD(P)H to specific salts related with the salinities remained poorly reported.

In our previous studies, ionic liquids with halide ions stimulated NADH in photobacteria (Zhang et al., 2013a,b; Yu et al., 2016a,b). Inorganic salts with halide ions (*e.g.*, sodium halide salts, NaX, X = F^-, Cl^-, Br^- and I^-) also stimulated on the NAD(P)H in photobacteria *Vibrio fischeri* (VF) (Yu et al., 2018). Moreover, simultaneous stimulations occurred in flavin mono-nucleotide (FMN), which is one essential reactants with NAD(P)H in the redox reactions (Jablonski and Deluca, 1978; Zhang et al., 2013a,b), and adenosine triphosphate (ATP), which is the essential energy in the FMN:NAD(P)H reactions (Blacker et al., 2014; Bao et al., 2015). These findings demonstrated an overall stimulation of salts with halide ions on the redox state. Yet, whether salts with different cations (*e.g.*, K^+, Ca^{2+} and Mg^{2+}) can result in similar redox responses remained to be answered.

Notably, the biochemical stimulations don't necessarily result in consistent apical outcomes (*e.g.*, luminescence in photobacteria). For example, [emim]Cl stimulated NAD(P)H were earlier than on luminescence, and [emim]Br stimulated NAD(P)H without any stimulation on luminescence (Yu et al., 2016a,b). Another example is that, the stimulations of sodium halide salts on luminescence were significantly higher than those on biochemical indicators (Yu et al., 2018), while those of [emim]Cl on luminescence were significantly lower than the biochemical stimulations on the same photobacteria (Yu et al., 2016a,b). The effects of cations on the consistency remained wide open to be explored.

In the present study, VF were incubated with KCl, $CaCl_2$ and $MgCl_2$. These cations were chosen because of their wide existence in the environment (Wei et al., 2016). The photobacteria VF was chosen due to its tolerance to high salinity (Soto et al., 2009) and its success in testing biochemical effects (Yu et al., 2016a,b; Yu et al., 2018). The NAD(P)H, together with FMN and ATP, were measured in a time-dependent fashion. The FMN:NAD(P)H reaction catalyst, luciferase (in the form of expression levels *lux* A and *lux* B (Yu et al., 2015)) and ATP regulating gene *adk* (Ping et al., 2013), were also measured at the same time. Subsequently, the luminescence effects were determined to confirm the apical outcomes. Our results demonstrated the common stimulatory effects of halide salts with chosen cations, and indicated their potential ecological disturbances.

2. Method and materials

2.1. Chemicals

Potassium chloride (KCl, CAS-RN: 7447-40-7), magnesium chloride ($MgCl_2$, CAS-RN: 7791-18-6), and calcium chloride ($CaCl_2$, CAS-RN: 10043-52-4) were purchased from Sigma-Aldrich Co. LLC. All stocking solutions were prepared and diluted with Milli-Q water containing 3% NaCl (approximately 0.51 mol/L) as a background salinity mimicking the seawater, and therefore all salt concentrations (expressed as nominal ones) in the present study were excessive to VF.

2.2. Bacterial culture

The freeze-dried VF was purchased from ATCC (USA). First, the complete liquid medium was prepared as 1.0 g yeast extract, 5.0 g tryptone, 1.0 g beef extract and 24.0 g NaCl in 1.0 L synthetic seawater (see reference (Yu et al., 2016a,b)). Before autoclavation at 121 °C for 20 min, the pH of the medium was adjusted to 7.4–7.6. Then, the photobacteria was resuscitated in the complete liquid culture medium with a shaking speed of 120 rpm at 30 ± 1 °C for 10–14 h allowing VF to reach the logarithmic growth phase. Next, the complete medium with VF was mixed with equal volume of two-fold concentrated culture medium, which contained 2.0 g yeast extract, 10.0 g tryptone, 2.0 g beef extract and 0.02 g Fe_3PO_4 in 1.0 L Milli-Q water and whose pH was adjusted to 7.4–7.6 before autoclavation (Zhang et al., 2013a,b). The mixed culture medium was incubated for another 0.5–1 h, allowing VF to reach a second logarithmic growth phase. Then, the bacterial suspensions were ready for experiments.

2.3. Time-dependent exposure of Vibrio fischeri to salts in conical flasks

To obtain enough biomass for bioassays, incubation of VF with the testing salts were performed in sterile conical flasks (Zhang et al., 2013a,b; Yu et al., 2016a,b). Briefly, each flask contained 15 mL photobacterial suspensions and 15 mL Milli-Q water (as the control) or salt solutions. Each salt concentration and the control had three replicates (*i.e.*, 18 flasks in total). The pH values of the solutions in each flask were still around 7.2–7.6 which was still the optimal conditions for VF culture (Scheerer et al., 2006), making the chloride salts the only stress in the present study.

The flasks were incubated at 30 ± 1 °C with a shaking speed of 120 rpm/min. At 0.5, 8, 16 and 24 h, 4 mL solutions containing photobacterial suspensions and salt solutions from each flask were collected into a 15 mL sterile centrifuge tube (18 tubes in total), which was used in subsequent bioassays. At 8 and 24 h, another 4 mL from each flask was collected into a 15 mL sterile centrifuge tube (36 tubes in total at 8 and 24 h), which was used in subsequent determination on expression levels of chosen genes. The tubes were centrifuged at 2500×g for 5 min (20 °C). After the supernatants in each tube were carefully discarded, the pellet was re-suspended with 1.0 mL ice-cold phosphate buffered saline (PBS, 0.1 M, pH 7). Next, the re-suspended suspensions were transferred into 1.5 mL sterile centrifuge tubes. Then, the tubes were centrifuged at 5000×g for 5 min (4 °C), after which the supernatants were discarded and the pellets were stored in −80 °C until assayed.

2.4. Bioassays on Vibrio fischeri

The bioassays on VF were carried out according to our previous studies (Zhang et al., 2013a,b; Yu et al., 2015). In brief, the bacterial pellets were homogenized with pestles in ice bath and washed in ice-cold PBS. After a centrifugation at 5000×g for 5 min (4 °C), the supernatants were used to determine NADH, NADPH, FMN and ATP via the enzyme-linked immune-sorbent assay (ELISA) kits (R&D Systems, Inc., USA) according to the manufacturer's instructions. The total protein (TP) was also determined by ELISA kits, and was subsequently used to indicate biomass in each sample. Then, each biochemical indicator was represented in their proportions to the corresponding TP to eliminate the biomass differences among samples.

2.5. Relative quantification of expression levels of target genes

The expression levels of target genes were determined

according to earlier studies with some modifications (Offermann et al., 2009; Yu et al., 2015). Total RNA was isolated from the bacterial pellets with TRIzol reagent, and was used to synthesize cDNA according to the manufacturer's instruction of M-MLV, Promega. The cDNA samples went through the real-time polymerase chain reaction (PCR) using SYBR Green Master Mix on Applied Biosystems 7900HT Fast Real-Time PCR System (USA). The expression levels of the target genes were quantified using the $2^{-\triangle\triangle CT}$ method (Livak and Schmittgen, 2001). In this method, the CT values (cycle times in PCR) to satisfy the requirement of fluorescent intensities were measured for each target gene (x) and the reference gene (ref). The ΔCT was calculated as $\Delta CT = CT_x - CT_{ref}$, referring to difference between the target gene and the reference gene in each sample or control. A further ΔΔCT was calculated as $\Delta\Delta CT = \Delta CT_i - \Delta CT_0$, referring to the difference between the treatment (salt exposure) and the control. The amount of target gene was normalized to the reference gene (16s rRNA) and was calculated using the following formula: relative amount of target gene $= 2^{-\Delta\Delta CT}$. The primer pairs for *lux* A, *lux* B, *adk* and 16s rRNA are referred in our previous study (Yu et al., 2015).

2.6. Time-dependent tests on luminescence

The time-dependent microplate analysis on luminescence of VF was carried out according to our previous study (Zhang et al., 2013a,b). Briefly, each test chemical had 5 concentrations (the same with those in testing the biochemical indicators) and one control in three parallels, which were arranged in the center wells of the white 96-well opaque plates (Corning Corp., USA) to avoid possible edge effects. Each of the wells contained 100 μL different concentrations of salt solutions or Milli-Q water (as control), and 100 μL prepared VF suspensions. The microplate was incubated at 30 ± 1 °C. The relative luminescent unit (RLU) in each test well was determined at 0.5, 8, 16, and 24 h (Yu et al., 2016a,b). The optical density at 570 nm (OD_{570}) values in the microplate were measured to indicate the changes of bacterial growth (Yu et al., 2016a,b).

2.7. Data representation and statistical analysis

All the data in the exposure were represented as their percentages of the concurrent control (Yu et al., 2015). Through this way, the data in the control were normalized to 1.0. POC greater than 1.0 (i.e., 100%) means stimulation or up-regulation, while POC less than 1.0 means inhibition or down-regulation. The ANOVA was carried out among the results from experiments that were carried out independently for at least three times. The probability levels of 0.05 ($p < 0.05$) were considered statistically significant. The data in the figures were expressed as mean ± standard deviation (SD) in the figures.

3. Results and discussion

3.1. Stimulatory effects of KCl, $MgCl_2$ and $CaCl_2$ on NADH and NADPH

The effects of KCl, $MgCl_2$ and $CaCl_2$ on NADH in VF are shown in Fig. 1. In KCl, NADH was not significantly influenced at 0.5 h. At 0.096 and 0.034 mol/L of KCl, NADH increased when exposure time increased, resulting in maximum stimulation values at each concentration. The greatest maximum stimulation of KCl on NADH was 33.3% higher than the control ($p < 0.05$) at 0.034 mol/L at 24 h. In $MgCl_2$, NADH showed stimulatory response at all concentrations. At 0.082 mol/L, the stimulation of $MgCl_2$ on NADH increased with time and reached 74.4% higher than the control ($p < 0.05$) at 24 h, while there no significant time-dependent changes at other concentrations. In $CaCl_2$, NADH showed similar responses to those in $MgCl_2$, and the greatest maximum stimulation was 96.9% higher than the control ($p < 0.05$) at 0.094 mol/L at 24 h. Notably, the greatest maximum stimulation of NaCl on NADH was 68% higher than the control ($p < 0.05$) at 0.135 mol/L at 24 h (Yu et al., 2018). The greatest maximum stimulation on NADH followed an order of $CaCl_2 > MgCl_2 > NaCl > KCl$.

The effects of KCl, $MgCl_2$ and $CaCl_2$ on NADPH in VF are also shown in Fig. 1. In KCl at 0.034, 0.012 and 0.004 mol/L, NADPH was stimulated at later time points, and the greatest maximum stimulation was 41.6% higher than the control ($p < 0.05$) at 0.034 mol/L. In $MgCl_2$, NADPH was slightly stimulated at 0.5 h, and the stimulation increased over time. The greatest maximum stimulation of $MgCl_2$ on NADPH was 51.9% higher than the control ($p < 0.05$) at 0.082 mol/L at 24 h. In $CaCl_2$, NADPH showed stimulatory responses at all concentrations and time points. The greatest maximum stimulation on NADPH were 122% higher than the control ($p < 0.05$) at 0.033 mol/L at 24 h. In NaCl, the greatest maximum stimulation on NADPH was 44% higher than the control ($p < 0.05$) at 0.135 mol/L at 24 h (Yu et al., 2018). The greatest stimulation on NADPH followed the order of $CaCl_2 \gg MgCl_2 > NaCl > KCl$, which was similar to that in NADH results.

The ratios of NADH to NADPH (NADH:NADPH) are listed in Table 1. In KCl, the NADH:NADPH ratios were generally around 1.0 and remained stable over time. In $MgCl_2$, the NADH:NADPH ratios were generally higher than 1.0, indicating that the stimulation on NADH was higher than that on NADPH. Especially at 0.223 mol/L, the NADH:NADPH ratio increased from 1.24 to 1.46 from 0.5 to 24 h. In $CaCl_2$, the NADH:NADPH ratios showed clear time-dependent decreases over time. For example, the NADH:NADPH ratio at 0.255 mol/L decreased from 1.26 to 0.83 from 0.5 to 24 h. Notably, the NADH:NADPH ratios in NaCl were higher than 1.0 with a first-increase from 0.5 to 8 h and a later-decrease from 8 to 24 h (Yu et al., 2018). The results of NADH:NADPH ratios did not show any particular pattern among the salts with different cations.

The stimulatory effects of NaCl, KCl, $MgCl_2$ and $CaCl_2$ on NAD(P)H indicated their common capacities to influence the energy production, biosynthetic and antioxidant responses via the redox disturbances (Ying, 2008; Collins et al., 2012). The increases in NADPH and decreases in the NADH/NADPH ratios resulted in higher metabolic activities and energy production/storage (Bao et al., 2015). The metabolic changes supported the adaptive responses of organisms to challenging salinities (Srivastava et al., 2008; Camejo et al., 2013).

3.2. Stimulatory effects of KCl, $MgCl_2$ and $CaCl_2$ on the overall redox reactions

The redox reaction of FMN:NAD(P)H is essential in providing energy for organisms to deal with challenging environment. The effects of KCl, $MgCl_2$ and $CaCl_2$ on FMN are shown in Fig. 1. In KCl, the stimulation on FMN increased when exposure time increased at 0.262, 0.096, 0.034 and 0.012 mol/L, and the greatest maximum stimulation at 24 h was 49.1% higher than the control ($p < 0.05$) at 0.034 mol/L. In $MgCl_2$, FMN was stimulated at all concentrations and time points. The stimulation increased over time at 0.082, 0.010 and 0.004 mol/L. The greatest maximum stimulation of $MgCl_2$ on FMN was 99.9% higher than the control ($p < 0.05$) at 0.082 mol/L at 24 h. In $CaCl_2$, the stimulation on FMN increased over time at 0.255, 0.094, 0.033 and 0.012 mol/L. The greatest maximum stimulation was 143% higher than the control ($p < 0.05$) at 0.094 mol/L at 24 h. The greatest maximum stimulation on FMN followed an order of $CaCl_2 > MgCl_2 > KCl$, which was similar to those in results of NAD(P)H.

Since both FMN and NAD(P)H showed stimulatory responses to

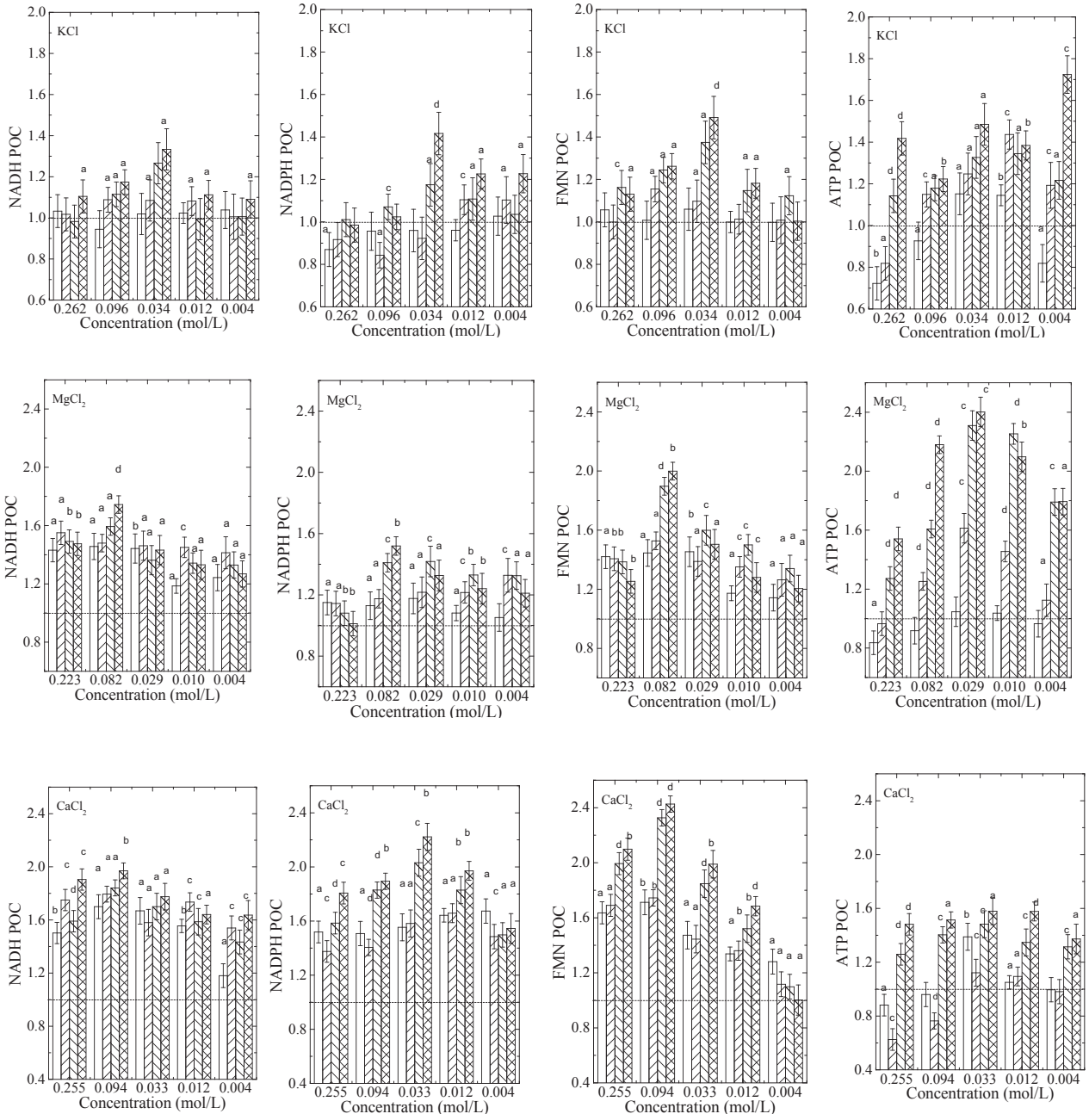

Fig. 1. The time-dependent toxicity of KCl, $MgCl_2$, and $CaCl_2$ on relative biochemical contents of *Vibrio Fischeri*. □: 0.5 h; ▨: 8 h; ▨: 16 h; ▨: 24 h. (a) Significantly different from the control; (b) significantly different from the control, and from the lower concentration; (c) significantly different from the control, and from the earlier time point in the same concentration; (d) significantly different from the control, from the lower concentration, and from the earlier time point in the same concentration. The data in the figures were represented as mean ± standard deviation.

KCl, $MgCl_2$ and $CaCl_2$, the luciferase that is the FMN:NAD(P)H reaction catalyst was assumed to be up-regulated. Accordingly, the relative expression levels of *lux* A and B that encode luciferase were analyzed, and the results are shown in Fig. 2. For *lux* A, the greatest up-regulation levels were 133%, 169%, and 205% higher than the control ($p < 0.05$) in KCl, $MgCl_2$, and $CaCl_2$, respectively. For *lux* B, the greatest up-regulation levels were 116%, 163%, and 172% higher than the control ($p < 0.05$) in KCl, $MgCl_2$, and $CaCl_2$, respectively. The up-regulation levels of *lux* A and *lux* B also followed the order of $CaCl_2 > MgCl_2 >$ KCl, which was in accordance with those in FMN and NAD(P)H.

The reactants and the catalyst in FMN:NAD(P)H reactions showed simultaneous stimulation, which inevitably would increase the energy supply in the organism. ATP is one ubiquitous energy form in all living bacterial cells, and is rapidly lost from dead cells (Shama and Malik, 2013). In this study, both ATP and the expression levels of *adk* gene (encoding enzymes to catalyze ATP generation) were measured. In KCl (Fig. 1), ATP was first inhibited at all concentrations and then stimulated over time, and the stimulation was generally the greatest at the lowest concentration. The greatest maximum stimulation of KCl on ATP was 72.3% higher than the control ($p < 0.05$) at 0.004 mol/L at 24 h. In $MgCl_2$ and $CaCl_2$, ATP showed similar time-dependent change to that in KCl, despite of different concentration-dependent pattern. The greatest maximum

Table 1
The content ratio of NADH to NADPH (NADH/TP:NADPH/TP) after the time-dependent exposure to NaCl, KCl, $MgCl_2$ and $CaCl_2$[a].

Chemicals	Time point (h)	Highest Con.*	Second Highest Con.	Medium Con.	Second lowest Con.	Lowest Con.
KCl	0.5	1.12	1.12	1.11	0.93	0.94
	8	1.13	1.15	1.12	0.99	0.89
	16	1.01	1.01	1.01	0.98	0.97
	24	1.13	1.17	1.11	1.04	0.98
$MgCl_2$	0.5	1.24	1.29	1.22	1.09	1.18
	8	1.36	1.27	1.21	1.20	1.07
	16	1.38	1.13	0.96	1.01	1.00
	24	1.46	1.16	1.09	1.07	1.06
$CaCl_2$	0.5	1.26	1.31	1.15	1.00	0.98
	8	1.27	1.28	1.00	1.05	1.04
	16	1.01	1.01	0.84	0.87	0.96
	24	0.83	0.89	0.75	0.79	0.76

[a] The exposure concentrations of KCl were 0.262, 0.096, 0.034, 0.012 and 0.004 mol/L. Those of $MgCl_2$ were 0.223, 0.082, 0.029, 0.010 and 0.004 mol/L. Those of $CaCl_2$ were 0.255, 0.094, 0.033, 0.012 and 0.004 mol/L. Blue shadow and the depth of the blue color indicated values higher than 1.0 and the distance from 1.0; red shadow and the depth of the red color indicated values higher than 1.0 and the distance from 1.0.

stimulation of $MgCl_2$ on ATP was 140% higher than the control ($p < 0.05$) at 0.029 mol/L at 24 h. The stimulations of $CaCl_2$ on ATP were similar among concentrations, ranging around 48.1%–57.9% at 24 h. The greatest maximum stimulation on ATP followed an order of $MgCl_2 > KCl > CaCl_2$. The stimulatory effects of KCl and $MgCl_2$ on ATP were greater at lower concentrations, while those of $CaCl_2$ were much less when compared with their results on FMN and NAD(P)H. In expression results of *adk* (Fig. 2), the up-regulation levels were the least in $CaCl_2$ (156%) compared with those in KCl (208%) and $MgCl_2$ (235%), following an order of $MgCl_2 > KCl > CaCl_2$ which was consistent with the ATP stimulation results.

Notably, FMN did not always show consistent results with NAD(P)H despite of their close connection in FMN:NAD(P)H redox reactions (Jablonski and Deluca, 1978; Zhang et al., 2013a,b). For example, the greatest maximum stimulation of KCl on FMN was similar to those on NAD(P)H. The greatest maximum stimulations of $MgCl_2$ and $CaCl_2$ on FMN were significantly higher than those on NAD(P)H (Fig. 1). Such inconsistency was also observed in the effects of halide salts and ionic liquids where the FMN:NAD(P)H ratio changed over time (Zhang and Liu, 2015; Yu et al., 2018). Such results indicated that FMN responded or consumed by NAD(P)H at different reaction rate (Zhang and Liu, 2015). Yet, the exact reason still needed further studies. At the same time, ATP and the up-regulation levels of its regulating gene did not show consistent results with FMN or NAD(P)H. It is well known that ATP was consumed in activities including *trans*-membrane transport, development, antioxidant reaction and damage repair (Agalakova and Gusev, 2012). Such wide consumption of ATP might have hindered the observation of its abrupt bust, and further studies are needed.

3.3. Influence of KCl, $MgCl_2$ and $CaCl_2$ on apical luminescence

The time-dependent effects of KCl, $MgCl_2$ and $CaCl_2$ on luminescence are shown in Fig. 3. In KCl, the luminescence was inhibited at 0.5 h, while the inhibition decreased and changed to stimulation at later time points at all concentrations and the stimulation increased with time. The greatest maximum stimulation was as high as 12.2-fold of the control ($p < 0.05$). In $MgCl_2$, the luminescence was inhibited at all time points at 0.223 mol/L, while the luminescence at other concentrations showed similar time-dependent changes to those of KCl. The greatest maximum stimulation of $MgCl_2$ was as high as 8.57-fold of the control ($p < 0.05$). In $CaCl_2$, the luminescence showed mostly inhibition, and it showed time-dependent stimulation at 0.033 and 0.012 mol/L. The greatest maximum stimulation was 2.0-fold of the control ($p < 0.05$). In NaCl, the greatest maximum stimulation was 10.12-fold of the control ($p < 0.05$) at 0.048 mol/L (Yu et al., 2018). According to the greatest maximum stimulation on luminescence, the salts followed an order of $KCl > NaCl > MgCl_2 > CaCl_2$, which was the opposite to the order in NAD(P)H and FMN and also different from those in ATP. Such inconsistence indicated complex biological processes between the redox reaction and the apical responses.

The biochemical and apical results demonstrated common stimulatory effects of chloride salts on the overall status of organisms, which indicated their common abilities to influence the adaptation of organisms and disturb their evolution and ecological stability (Costantini et al., 2010; Yu et al., 2018). The FMN:NAD(P)H resultant luminescence was an important means to counterbalance the oxidative stress that was caused by the intra- or extracellular oxygen concentrations. Such responses are essential in the evolution of bacteria from anaerobic to aerobic environments (Bose et al., 2007).

Notably, the significant increases in luminescence was not accompanied with increases in bacterial growth according to non-significant changes in OD_{570} values (data not shown). Such effects indicated the involvement of quorum sensing (QS). The responses of QS demonstrated the power of the individual needs in driving the evolution of a regulatory pattern that provides the optimal function for the whole bacterial species and also the host-microbe associations (Miyashiro and Ruby, 2012). The involvement of QS in the present study suggested that salinities not only influence the bacterial species but also its host species, and therefore have potentials to disturb the marine ecosystems. The salinities in the ocean showed significant changes since the last deglaciation

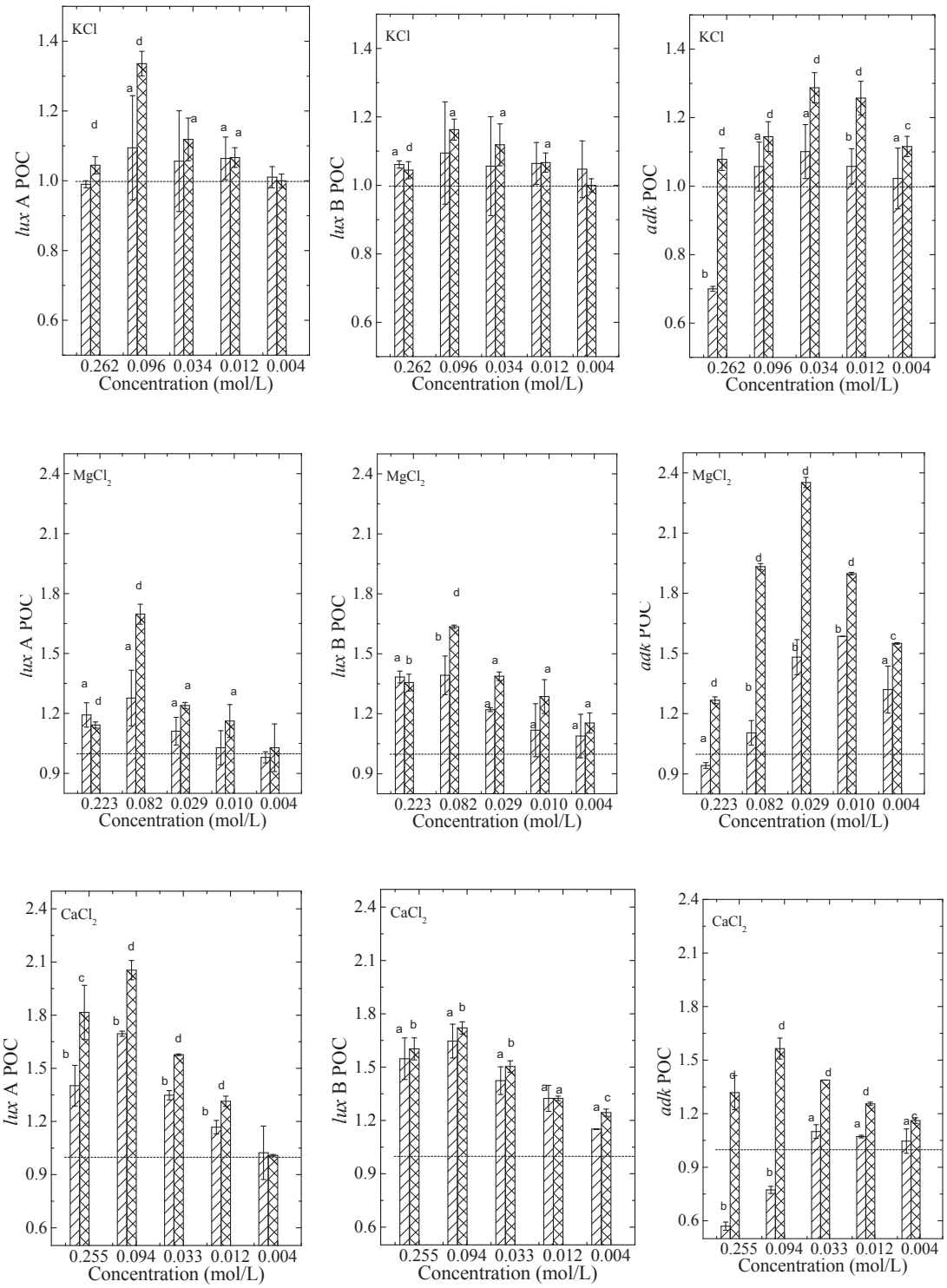

Fig. 2. The time-dependent effects of KCl, $MgCl_2$, and $CaCl_2$ on expression levels of *lux* A, *lux* B and *adk* in *Vibrio fischeri*. ▨: 8 h; ▩: 24 h. POC: percentage of control; a: Significantly different from the control; b: significantly different from the control, and from the lower concentration; c: significantly different from the control, and from the earlier time point in the same concentration; d: significantly different from the control, from the lower concentration, and from the earlier time point in the same concentration. The data in the figures were represented as mean ± standard deviation.

(Warden et al., 2016). The salinities would further change due to mineral mining, wastewater irrigation and effluent discharge from seawater usage for drinking water treatment, and also from snow melting and seawater intrusion during the global climate change (Singh, 2015; Bloetscher et al., 2016; Wei et al., 2016; Stancanelli et al., 2017). Therefore, the present finding demonstrated an ecological concern on the increasing concentrations of inorganic salts due to anthropogenic activities and climate change.

4. Conclusion

Incubation with KCl, $MgCl_2$ and $CaCl_2$ stimulated NADH and

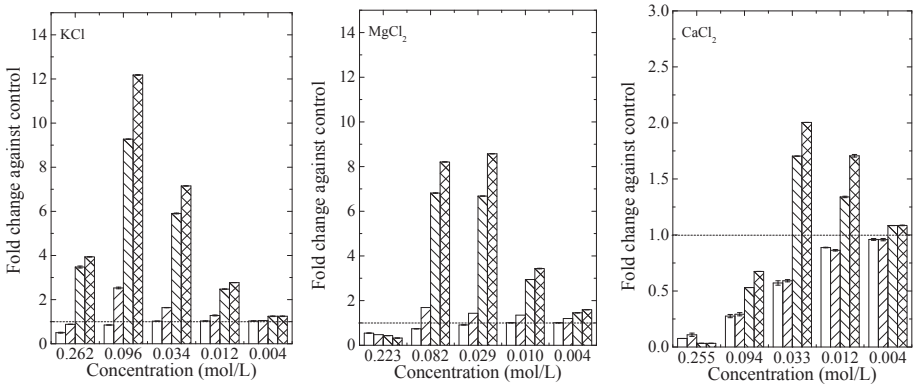

Fig. 3. The time-dependent effects of KCl, $MgCl_2$, and $CaCl_2$ on luminescence of *Vibrio fischeri*. ▭: 0.5 h; ▨: 8 h; ▧: 16 h; ▩: 24 h. Since the data in the exposure were significantly higher than those in the control, they were transformed from percentage of control (POC) to fold-change against the control.

NADPH in *Vibrio fischeri* in a time-dependent fashion. The greatest maximum stimulation on NAD(P)H at 24 h followed an order of $CaCl_2 > MgCl_2 > KCl$. The changes of NADH:NADPH ratios over time in $CaCl_2$, $MgCl_2$ and KCl were descendent, ascendant and stable, respectively. The NAD(P)H results indicated energy consumption changes in the adaptive responses. At the same time, FMN and ATP were stimulated with up-regulation on FMN:NAD(P)H redox reaction catalyst (luciferase, in the form of *lux* A and *lux* B) and ATP regulating gene *adk*. The overall stimulation on the redox reaction resulted in even more significant stimulation on the apical luminescence. The present findings urged ecological concerns on the salinity changes due to anthropogenic activities and climate change.

Acknowledgements

This work was supported by National Research Council of Science and Technology Major Project for Water Pollution Control and Treatment (2017ZX07201004), Guangxi Key Laboratory of Electrochemical and Magnetochemical Functional Materials (EMFM20182206) and National Natural Science Foundation of China (No. 21407061). The authors are sincerely grateful for their financial support.

References

Agalakova, N.I., Gusev, G.P., 2012. Fluoride induces oxidative stress and ATP depletionin the rat erythrocytes *in vitro*. Environ. Toxicol. Pharmacol. 34, 334–337.
Bao, T., Zhang, X., Zhao, X., Rao, Z., Yang, T., Yang, S., 2015. Regulation of the NADH pool and NADH/NADPH ratio redistributes acetoin and 2,3-butanediol proportion in *Bacillus subtilis*. Biotechnol. J. 10, 1298–1306.
Blacker, T.S., Mann, Z.F., Gale, J.E., Ziegler, M., Bain, A.J., Szabadkai, G., Duchen, M.R., 2014. Separating NADH and NADPH fluorescence in live cells and tissues using FLIM. Nat. Commun. 5, 3936.
Bloetscher, F., Polsky, C., Bolter, K., Mitsova, D., Garces, K.P., King, R., Carballo, I.C., Hamilton, K., 2016. Assessing potential impacts of sea level rise on public health and vulnerable populations in southeast Florida and providing a framework to improve outcomes. Sustainability 8, 315–322.
Bose, J.L., Kim, U., Bartkowski, W., Gunsalus, R.P., Overley, A.M., Lyell, N.L., Visick, K.L., Stabb, E.V., 2007. Bioluminescence in Vibrio fischeri is controlled by the redox-responsive regulator ArcA. Mol. Microbiol. 65, 538–553.
Camejo, D., Romero-Puertas, M.d.C., Rodríguez-Serrano, M., MaríaSandalio, L., Lázaro, J.J., Jiménez, A., Sevilla, F., 2013. Salinity-induced changes in S-nitrosylation of pea mitochondrial proteins. J. Proteomics 79, 87–99.
Collins, Y., Chouchani, E.T., James, A.M., Menger, K.E., Cochemé, H.M., Murphy, M.P., 2012. Mitochondrial redox signalling at a glance. J. Cell Sci. 125, 801–806.
Costantini, D., Metcalfe, N.B., Monaghan, P., 2010. Ecological processes in a hormeticframework. Ecol. Lett. 13, 1435–1447.
Dugo, G., Pellicanò, T.M., Pera, L.L., Turco, V.L., Tamborrino, A., Clodoveo, M.L., 2007. Determination of inorganic anions in commercial seed oils and in virgin olive oils produced from de-stoned olives and traditional extraction methods, using suppressed ion exchange chromatography (IEC). Food Chem. 102, 599–605.
Fahmi, A.I., Nagaty, H.H., Eissa, R.A., Hassan, M.M., 2011. Effects of salt stress on some nitrogen fixation parameters in faba bean. Pakistan J. Biol. Sci. 14, 385–391.
Gonçalves-de-Albuquerque, C.F., Silva, A.R., da Silva, C.I., Castro-Faria-Neto, H.C., Burth, P., 2017. Na/K pump and beyond: Na/K-ATPase as a modulator of apoptosis and autophagy. Molecules 22, 578–595.
Jablonski, E., Deluca, M., 1978. Studies of the control of luminescence in *Beneckea harveyi*: properties of the NADH and NADPH: FMN oxidoreductases. Biochemistry 17, 672–678.
Livak, K., Schmittgen, T., 2001. Analysis of relative gene expression data using real-time quantitative PCR and the $2^{-\Delta\Delta CT}$ method. Methods 25, 402–408.
Luo, Y., Roux, B., 2010. Simulation of osmotic pressure in concentrated aqueous salt solutions. J. Phys. Chem. Lett. 1, 183–189.
Miyashiro, T., Ruby, E.G., 2012. Shedding light on bioluminescence regulation in *Vibrio fischeri*. Mol. Microbiol. 84, 795–806.
NRC (National Research Council), 2006. Fluoride in Drinking Water: Scientific Review of EPA's Standards. National Academies Press, Washington, DC. USA.
Offermann, K., Matthäi, A., Ahlf, W., 2009. Assessing the importance of dietborne-cadmium and particle characteristics on bioavailability and bioaccumulationin the nematodes *Caenorhabditis elegans*. Environ. Toxicol. Chem. 28, 1149–1158.
Ping, J., Hao, P., Li, Y.-X., Wang, J.-F., 2013. Molecular dynamics studies on the conformational transitions of adenylate kinase: a computational evidence for the conformational selection mechanism. BioMed Res. Int. 2013, 628536.
Scheerer, S., Gomez, F., Lloyd, D., 2006. Bioluminescence of Vibrio fischeri in continuous culture: optimal conditions for stability and intensity of photoemission. J. Microbiol. Meth. 67, 321–329.
Shama, G., Malik, D.J., 2013. The uses and abuses of rapid bioluminescence-based ATP assays. Int. J. Hyg. Environ. Health 216, 115–125.
Singh, A., 2015. Managing the environmental problem of seawater intrusion in coastal aquifers through simulation-optimization modeling. Ecol. Indicat. 48, 498–504.
Soto, W., Gutierrez, J., Remmenga, M.D., Nishiguchi, M.K., 2009. Salinity and temperature effects on physiological responses of *Vibrio fischeri* from diverse ecological niches. Microb. Ecol. 57, 140–150.
Srivastava, A.K., Bhargava, P., Thapar, R., Rai, L.C., 2008. Salinity-induced physiological and proteomic changes in *Anabaena doliolum*. Environ. Exp. Bot. 64, 49–57.
Stancanelli, L.M., Musumeci, R.E., Cavallaro, L., Foti, E., 2017. A small scale Pressure Retarded Osmosis power plant: dynamics of the brackish effluent discharge along the coast. Ocean Eng. 130, 417–428.
Warden, L., van der Meer, M.T.J., Moros, M., Damsté, J.S.S., 2016. Sedimentary alkenone distributions reflect salinity changes in the Baltic Sea over the Holocene. Org. Geochem. 102, 30–44 (Tokyo. 1967).
Wei, H., Wu, J.-k., Shen, Y.-p., Zhang, W., Liu, S.-w., Zhou, J.-x, 2016. Hydrochemical characteristics of snow meltwater and river water during snow-melting period in the headwaters of the Ertis River. Xinjiang. Environ. Sci. 37, 1345–1352.
Ying, W., 2008. NAD^+/NADH and $NADP^+$/NADPH in cellular functions and cell death: regulation and biological consequences. Antioxidants Redox Signal. 10, 179–206.
Yu, Z., Zhang, J., Hou, M., 2018. The time-dependent stimulation of sodium halide salts on redox reactants, energy supply and luminescence in *Vibrio fischeri*. J. Hazard Mater. 342, 429–435.
Yu, Z., Zhang, J., Liu, S., 2015. Biochemical and gene expression effects of 1-alkyl-3-methylimidazolium tetrafluoroborate on *Vibrio qinghaiensis* sp.-Q67. J. Hazard Mater. 300, 483–492.
Yu, Z., Mo, L., Zhang, J., Liu, S., 2016a. Time- and anion-dependent stimulation on triphosphopyridine nucleotide followed by antioxidant responses in *Vibrio fischeri* after exposure to 1-ethyl-3-methylimidazolium salts. Chemosphere 163, 452–460.
Yu, Z., Zhang, J., Yin, D., 2016b. Multigenerational effects of heavy metals on feeding, growth, initial reproduction and antioxidants in Caenorhabditis elegans. PLoS

One 11, e0154529.
Zhang, J., Liu, S., 2015. Time-dependent stimulations of 1-alkyl-3-methylimidazolium chloride on redox reactants and antioxidases in *Vibrio qinghaiensis* sp.-Q67. J. Hazard Mater. 283, 568–573.
Zhang, J., Liu, S., Yu, Z., Zhang, J., 2013a. Time-dependent hormetic effects of 1-alkyl-3-methylimidazolium bromide on *Vibrio qinghaiensis* sp.-Q67: luminescence, redox reactants and antioxidases. Chemosphere 91, 462–467.
Zhang, J., Liu, S.S., Yu, Z.Y., Ge, H.L., Zhang, J., 2013b. The time-dependent hormetic effects of 1-alkyl-3-methylimidazolium chloride and their mixtures on *Vibrio qinghaiensis* sp. -Q67. J. Hazard Mater. 258–259, 70–76.